

Dielectric properties and thermal conductivity of graphene nanoplatelet filled poly(vinylidene fluoride) (PVDF)/poly(methyl methacrylate) (PMMA) blend

Dandan Yang¹ · Haiping Xu¹ · Wei Yu¹ · Jingrong Wang¹ · Xianchen Gong¹

Received: 4 April 2017 / Accepted: 12 May 2017 / Published online: 16 May 2017
© Springer Science+Business Media New York 2017

Abstract Poly(methyl methacrylate) (PMMA) and graphene nanoplatelet (GNP) was introduced into poly(vinylidene fluoride) (PVDF) via a solution blending process, and a series of PVDF/PMMA/GNP composites were obtained. Scanning electron microscope (SEM) micrographs of the composite with 4 wt% GNP loading showed that GNP randomly dispersed and partly arranged parallel to each other in the matrix. Fourier transform infrared (FT-IR) spectroscopy results and X-ray diffraction (XRD) analysis revealed the increasing percentage of β - and γ -phase PVDF crystals in the composites with increasing the GNP contents. The frequency dependent electrical conductivity and dielectric properties of composites have been performed in the range of 10^2 – 10^7 Hz which obeyed the percolation theory. Dielectric constant and dielectric loss of composites increased with increasing GNP contents in the all frequency region. A dielectric constant of ~ 148 and dielectric loss of ~ 0.3 was observed at 10^2 Hz with 4 wt% of GNP loading, which is near the percolation threshold. Meanwhile, the thermal conductivity reached up to 0.84 W/m K for PVDF/PMMA/GNP composites with 4 wt% of GNP loading. An approach was provided to develop a variety of highly thermally conductive dielectric materials.

1 Introduction

Dielectric materials with high dielectric constant, low dielectric loss and light weight are significantly needed for many practical applications in energy storage devices, transducers and electromechanical actuators [1–5]. Nowadays, demands have become more and more stringent for dielectric materials. Furthermore, there has been an increasing demand for handling the issue of thermal management in electronic equipments [6, 7]. Traditional ceramic dielectric materials can hardly meet all the requirements for dielectric and thermal properties for specific applications [8]. There is increasing interest in development of conductive and dielectric nanostructured polymeric materials based on graphene for a wide range of applications [9–11]. Graphene has high aspect ratio, high electrical and thermal conductivities, and remarkable tensile properties. Graphene-based polymer composites show not only outstanding mechanical properties but also remarkable functional properties, such as easy processing, flexibility, light weight, good electrical and thermal conductivity, unique photonic/optical transportation, anisotropic transport, superior environmental resistance, and so on [12–15]. In polymer nanocomposites, multi-sheet graphene, known as graphene nanoplatelets (GNPs), is more favorable because of its cost advantage over single-sheet graphene and carbon nanotubes (CNTs), since it can be obtained by simple exfoliation of graphite [16, 17].

Poly(vinylidene fluoride) (PVDF), a semicrystalline polymer, shows excellent mechanical properties, high thermal and chemical stability, advantageous piezo- and pyro-electric properties. It exists in a number of crystalline forms, i.e. the antipolar α -form with a TGTG' molecular conformation, the polar β -form with all *trans*-TTT

✉ Dandan Yang
ddyang@sspu.edu.cn

✉ Haiping Xu
hpxu163@163.com

¹ School of Environmental and Materials Engineering,
Shanghai Polytechnic University, 2360 Jinhai RD, Pudong,
Shanghai 201209, People's Republic of China

planar zig-zag conformation, and a third crystalline form known as the γ -form with a T_3GT_3G' conformation, usually obtained from solution-cast films [18]. The non-polar α -phase is the most common form with the *trans-gauche-trans-gauche'* (TGTG') conformation, as well as excellent mechanical properties. These properties make α -phase PVDF a good electro-optical storage material, which can be used for specific optical, electronic and solar energy devices. The β -phase has the largest spontaneous polarization per unit cell and the γ -phase ranks second, thus providing the piezoelectric properties. PVDF is highly miscible with oxygen-containing hydrophilic polymers such as poly(vinyl pyrrolidone) (PVP), poly(vinyl acetate) (PVAc) and poly(methyl methacrylate) (PMMA) [19–21], which is related to the interaction between the fluorine atoms and carbonyl groups of the partner. Among these polymers, PMMA is more interesting due to its strong compatibility with PVDF all over the concentration range in the blend polymer. Abdelaziz [22] and Zhang et al. [23] investigated that the presence of PMMA was in favor of the β -phase transformation, but higher blending degree of PMMA could not increase the formation of β -phase further. In our previous study [24], we displayed the dielectric performance of PVDF/PMMA/hydroxylated multiwall carbon nanotubes (MWNTs–OH) composites. It has already been demonstrated that the introduction of even a small fraction of MWNTs–OH component can dramatically improve the dielectric performance of the PVDF/PMMA blends. However, two-dimensional (2D) geometry GNPs are not as effective as one-dimensional (1D) MWNTs–OH in forming conductive networks in PVDF/PMMA blends. Thus, GNP-filled composites are expected to have higher electrical percolation threshold and lower electrical conductivity than MWNTs–OH-filled composites. Nonetheless, the 2D geometry of GNPs is suitable for energy storage applications, and the anisotropic electrical and thermal properties of GNPs are considered advantageous for applications in batteries, conductive coatings, sensors, and electromagnetic interference shielding materials etc. [25, 26]. Herein, the microstructure, alternate-current (ac) electrical conductivity, dielectric characteristics and thermal conductivity of PVDF/PMMA/GNP composites were investigated in the present study. The PVDF/PMMA blend with the mass ratio of 70/30 is selected as the polymer matrix, which exhibits the best balance of hydrophilicity, hardness, mechanical strength, and so on [23]. At a 4 wt% GNP content, the dielectric constant and thermal conductivity reached 148 and 0.84 W/m K for PVDF/PMMA/GNP composite, respectively. Our finding provides a path to develop a variety of highly thermally conductive dielectric materials with low-cost.

2 Experimental procedure

2.1 Materials

PVDF (FR903, the melt index is 2.0 g/10 min) material in powder form was obtained from Shanghai 3F New Materials Ltd, China. PMMA material (low molecular weight) was obtained from Nantong Liyang Chemical Co., Ltd, China. The GNP used as conductive filler was provided by Nanjing Ji Cang Nano Tech Co., Ltd with the average thickness of 100–200 nm. *N,N*-dimethylformamide (DMF) was purchased from Sinopharm Chemical Reagent Co., Ltd, China. All the chemicals were used as received.

2.2 Preparation

Firstly, both PVDF and PMMA were dissolved in an organic solvent DMF, separately. The polymer blend of PVDF and PMMA with mass ratio of 70/30 was prepared via a solution mixing and casting technique. GNPs were also dispersed in DMF by bath-sonicating for 50 min. Then, the suspension of GNPs in DMF was added into PVDF and PMMA solution. The mixtures of the dissolved polymers with the GNPs were stirred by ultrasonic treatment for 50 min and further magnetic stirring for 4 h. Consequently the mixture solution was cast onto a glass dish and dried at 80 °C for 24 h to minimize the solvent traces, then molded by hot pressing under 18 MPa at 190 °C for 20 min and slowly cooled to room temperature under the pressure. The final samples with a disk shape were 12 mm in diameter and 1 mm in thickness. Electrodes were painted with silver paste for electrical measurement. A series of PVDF/PMMA/GNP composites with various contents of GNPs were obtained.

2.3 Characterization

Microstructures of fractured surfaces of composites were observed by SEM (SEM, HITACHI S-4800, Japan). The samples were gold sputtered in vacuum prior to observation. XRD patterns of samples were carried out using Cu $K\alpha$ ($\lambda = 0.15406$ nm) radiation (XRD, Bruker D8-Advance, Germany). The FT-IR spectra of these samples were measured by Fourier transform infrared spectroscopy (FT-IR, Bruker V-70, Germany) in the wave number range 400–1450 cm^{-1} . The AC conductivity, dielectric constant and dielectric loss of the samples were determined by Novocontrol TOP Class Dielectric Spectrometer with an Alpha-A high performance analyzer (DBS-80, Germany) at room temperature in frequency ranging of 10^2 – 10^7 Hz. The working electrodes were prepared by painting silver paste on both sides of the samples. The thermal conductivity of the sample was obtained using the thermal

conductivity analyzer (C-Therm TCi, C-Therm Technologies, Canada), which is based upon a modified transient plane source method. The testing capabilities of the system are 0–100 W/m K across a wide range of temperature (–50 to 200 °C) and the accuracy of the instrument is better than 5%. All the thermal conductivity measurements of the samples in the experiments were repeated at least five times to ascertain the accuracy of the experimental results at room temperature.

3 Results and discussion

3.1 Morphological features and microstructure

Figure 1 shows the SEM micrographs of the GNP and 4 wt% GNP filled PVDF/PMMA composite. It is evident that the GNPs particles are randomly dispersed and have good adhesion within the PVDF/PMMA matrix. These GNP particles have irregular geometry with approximately equivalent diameter of a few microns (Fig. 1a). As shown in Fig. 1b, the absence of holes and voids at the GNPs and polymer interface indicates excellent adhesion between the GNPs and PVDF/PMMA matrix. No major agglomerates were observed from SEM analysis at micron scale, which reveals a good level of GNPs dispersion. It is also observed that PVDF and PMMA are compatible to a great extent, which is attributed to polar interactions between CF_2 and $\text{C}=\text{O}$ groups. From Fig. 1b one can observe that GNPs are entrapped into polymer matrix and arranged parallel to each other. The neighboring GNPs can be considered as electrode and a thin layer of polymer between them acts as the dielectric, forming numerous microcapacitors in the composites (Fig. 1c), which is in favor of the high dielectric constant in percolative composites.

FT-IR spectroscopy provides information about the complexation and interactions between the various constituents in the polymeric matrix. FT-IR spectra of PVDF/PMMA/GNP composites are shown in Fig. 2. It is well known that the main characteristic vibration peaks of the α -phase in PVDF are 410, 532, 764, 795, 855 and 978 cm^{-1} , of the β -phase in PVDF are 445, 510, 840, 878 and 1403 cm^{-1} , and of the γ -phase in PVDF are 430, 510, 811 and 1233 cm^{-1} [27–29]. For the PVDF/PMMA/GNP composites with 1 and 2 wt% GNP, the identified peaks at 764, 795, 855 and 978 cm^{-1} are assigned to presence of PVDF α -phase. And weak peaks at 430, 840 and 878 cm^{-1} can also be observed, which means that trace amounts of PVDF polar β - and γ -phase are also present in composites, as shown in Fig. 2. As loading of GNPs increase to 3 wt%, vibration peaks at 795, 855 and 978 cm^{-1} almost disappear, and 430, 510, 811, 840, 878 and 1403 cm^{-1} are notably observed, which means that the dominant phase is

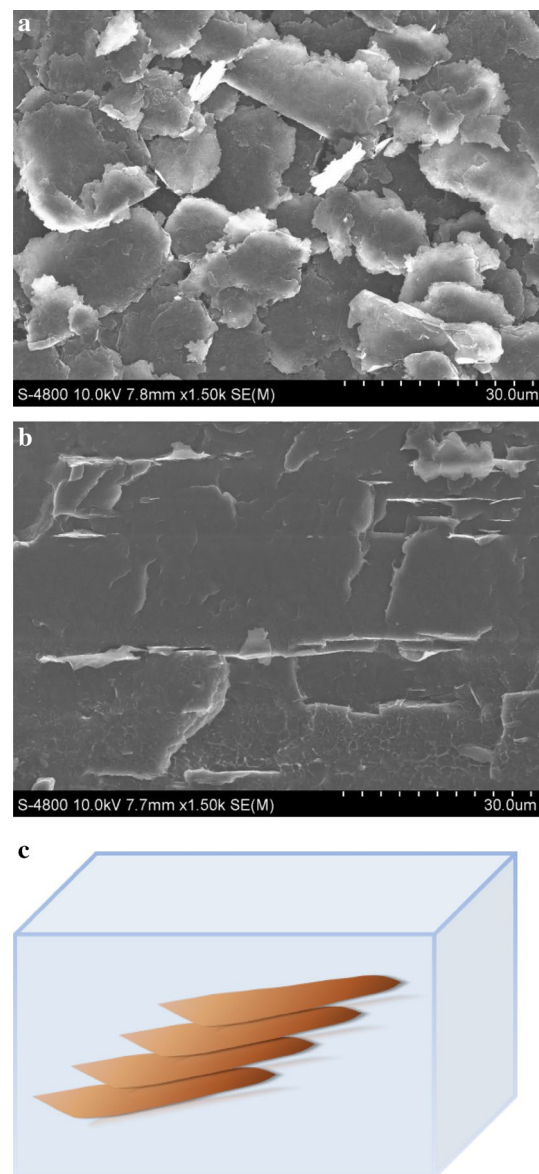


Fig. 1 SEM images of **a** GNP particles and **b** freeze fractured surface morphology of PVDF/PMMA/GNP composite with 4 wt% GNP loading, **c** schematic diagrams of the distribution of GNPs in the composites

the β - and γ -phase in PVDF/PMMA/GNP composites. The FT-IR technique is successfully used to quantify the variations of β - and γ -phase, and these results are confirmed by XRD analysis.

In order to examine the influence of PMMA and GNPs on the semicrystalline structure of PVDF, the X-ray diffraction patterns of neat PVDF, PVDF/PMMA blend and PVDF/PMMA/GNP composites are shown in Fig. 3. The spectrum of neat PVDF shows three discernible diffraction peaks appear at 18.4°, 20.0° and 26.7°, referent to the diffractions in planes (020), (110) and (021), respectively,

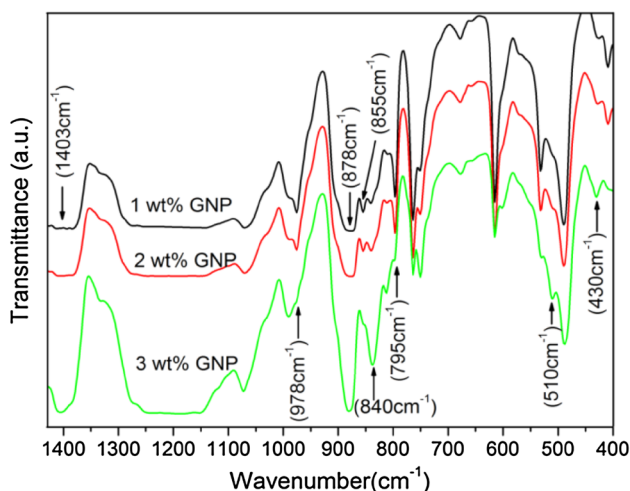


Fig. 2 FT-IR spectra of PVDF/PMMA/GNP composites, in which GNP content is 1, 2 and 3 wt%, respectively

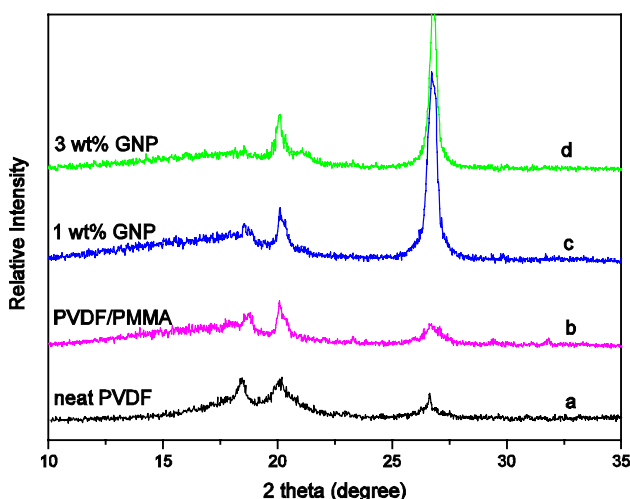


Fig. 3 XRD pattern of neat PVDF, PVDF/PMMA blend and PVDF/PMMA/GNP composites with GNP content is 1 and 3 wt%, respectively

all characteristic of the α -phase (Fig. 3a) [30, 31]. When PVDF is blended with PMMA, the reflections of (020), (101) and (200, 110) crystallographic planes of PVDF γ -phase and β -phase crystals are observed at 18.5°, 20.2° and 20.1°, respectively (Fig. 3b) [18]. From Fig. 3b, a broad double peaks appears around 20.1°–20.2°, which can be ascribed to the appearance of β -phase and γ -phase, but the two peaks are hard to distinguish from each other. Meanwhile, the peak intensity of α -phase crystal decreases (Fig. 3b), suggesting that the PMMA is able to interact with PVDF chains in the amorphous regions and at interphases to prohibit PVDF segments diffusion towards the crystallization fronts. When 1 wt% GNPs are filled into the blend, the intensification of double peaks at around

20.1°–20.2° indicates that the addition of small amount of GNPs can promote the molecules in PVDF to more regular, resulting in increased polar phase of PVDF (Fig. 3c). The diffraction peak at 26.5° is identified as GNPs (002) plane. From Fig. 3d, it is observed that by mixing of 3 wt% GNPs with PVDF/PMMA blend, the PVDF α -phase diffraction peaks get nearly disappeared and β -phase diffraction peaks at 20.1° become sharper than that of neat PVDF. From the FT-IR and XRD results it can be concluded that GNPs act as a nucleation agent for polar phase formation and its enhancement in PVDF, therefore, the PVDF composites acquired piezoelectric properties.

3.2 AC conductivity

Figure 4 shows AC conductivity of neat PVDF, PVDF/PMMA blend and PVDF/PMMA/GNP composites with various GNPs contents as a function of electric field frequency of 10²–10⁷ Hz at room temperature. It is found that AC conductivity of the composites is strongly dependent on the applied electric field frequency as well as the GNPs content. For the neat PVDF, PVDF/PMMA blend and composites with GNPs loading below 3 wt%, AC conductivity is not more than 10⁻⁸ S/cm at 10² Hz and it increased with the increment of the frequency. The low AC conductivity as well as its increasing trend with the electric field frequency demonstrates that the neat PVDF, PVDF/PMMA blend and composites with GNPs loading below 3 wt% are electrically insulating materials. The higher conductivity at higher frequencies confirms that the short range intra-well hopping of charge carriers between localized states. It can also be seen that the AC conductivity increase sharply to over 10⁻⁶ S/cm at 10² Hz when GNPs loading increase

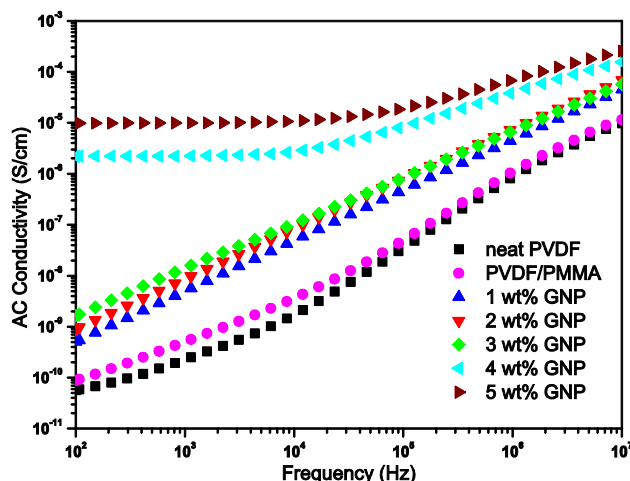


Fig. 4 Frequency dependence of AC conductivity for neat PVDF, PVDF/PMMA blend and PVDF/PMMA/GNP composites with various GNPs contents at room temperature

to over 4 wt%. Figure 4 indicates that the electrical conductivity increases with increasing the content of GNPs according to percolation theory. The percolation threshold is defined as a minimum concentration of the conducting filler at which a continuous conductive paths of macroscopic length appears in the system. Near the percolation threshold, the electrical conductivity and dielectric constant of the dielectric composites increase rapidly. From Fig. 4, the estimated percolation threshold value is located at nearly 4 wt% GNPs content.

3.3 Dielectric behavior

Figure 5 shows variation of dielectric constants of neat PVDF, PVDF/PMMA blend and PVDF/PMMA/GNP composites with various GNPs contents as a function of electric field frequency of 10^2 – 10^7 Hz at room temperature. Dielectric constants of the neat PVDF and PVDF/PMMA blend are 9–11, which remained constant irrespective with the applied electric field frequency. For PVDF/PMMA/GNP composites with low GNPs loading below 3 wt%, the dielectric constants are 15–50. When the content of GNPs was 4 wt%, the dielectric constant of composite increase rapidly to 148 at 10^2 Hz and it diminishes with the increment of the applied frequency. As shown in Fig. 5, when a small amount of GNPs (below 3 wt%) is incorporated into the polymer matrix, GNPs act as capacitor electrodes and some microcapacitance structures are formed, resulting in a slight increase of dielectric constant relative to that of pure polymer. At the percolation threshold content, a very thin dielectric insulating-polymer layer of polymer is sandwiched by two neighboring GNPs, and GNPs almost contact each other

but remained isolated and electrically insulated to form lots of parallel or serial microcapacitors, which leads to a high dielectric constant. Then, beyond the percolation threshold, the dielectric constant of the composite keeps on increasing, because GNPs are still wrapped by a thin layer of polymer matrix, if they are well dispersed. The good dispersion of graphene in the matrix and the parallel ‘microcapacitor’ structure could be found in the SEM (Fig. 1b, c) fraction image of the composite with the 4 wt% GNPs loading. As the GNPs content increase to 5 wt%, the number of ‘microcapacitor’ is increased, as well as conductive network is partly formed [32]. Consequently, the dielectric constant and AC conductivity of composite with 5 wt% GNPs slightly increase than those of composite with 4 wt% GNPs loading, as shown in Figs. 4 and 5.

Figure 6 presents the frequency dependence of dielectric loss for neat PVDF, PVDF/PMMA blend and PVDF/PMMA/GNP composites with various GNPs contents at room temperature. The values of dielectric loss tend to become higher and higher in the total frequency range considered with the increase of GNPs concentration for the composites. It is well known that the dielectric loss depends on the conducting nature of material, the incorporation of GNPs into blend increases composites’ conductivity, which seems to increase the dielectric loss of the composites as compared to neat PVDF and PVDF/PMMA blend. Combined with the results from Figs. 4 and 5, the aforementioned AC conductivities and dielectric constant results hint that the dielectric loss of the composites increase rapidly beyond the percolation threshold, owing to the formation of a small amount of GNPs conductive paths and the leakage current, as evident from the Fig. 6.

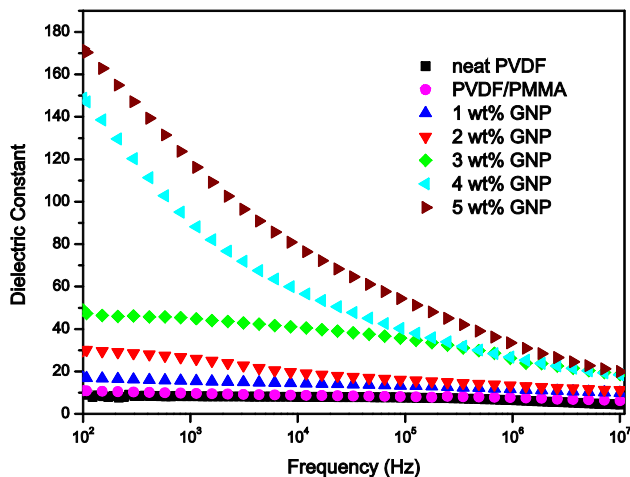


Fig. 5 Frequency dependence of dielectric constant for neat PVDF, PVDF/PMMA blend and PVDF/PMMA/GNP composites with various GNPs contents at room temperature

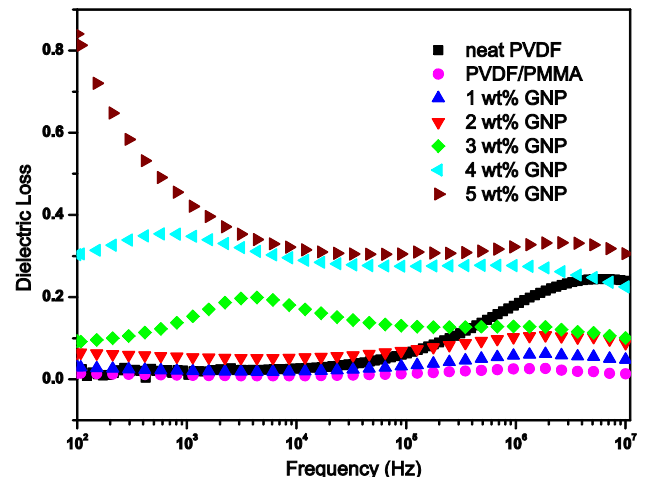


Fig. 6 Frequency dependence of dielectric loss for neat PVDF, PVDF/PMMA blend and PVDF/PMMA/GNP composites with various GNPs contents at room temperature

3.4 Thermal conductivity

The mass fraction of GNPs fillers affecting on the thermal conductivities of the composites is shown in Fig. 7. An observably thermal conductivity enhancement is indicated with increasing addition of GNPs fillers in composites (Fig. 7). The value of the composite with 4 wt% GNPs is improved to 0.84 W/m K, about 2.8 times that of pure PVDF (about 0.30 W/m K). Furthermore, thermal conductivity of the composite with 5 wt% GNP loading is 0.97 W/m K. It is suggested that an interconnected GNPs framework can be developed in the polymer matrix, leading to significant heat transfer enhancement of the composites. The variation trend of the composites' thermal conductivity is in agreement with that of electrical conductivity.

4 Conclusion

In conclusion, a study of the AC electrical, dielectric and thermal properties of PVDF/PMMA/GNP composites is carried out in different measuring conditions of frequency and GNPs concentration. XRD and FT-IR results demonstrate that GNPs promote the formation of polar-phase crystals in PVDF. SEM images of PVDF/PMMA/GNPs composite confirm that GNPs are dispersed uniformly in the matrix. It is found that the frequency-dependent AC electrical conductivity of the composites is strongly dependent on the GNPs content. The percolation threshold value locates at about 4 wt% GNPs concentration. The results showed that the dielectric constant and dielectric loss of composites increase with rising GNPs content. The enhancement dielectric constant can be explained according to the formation of numerous “microcapacitance” structure. It is also

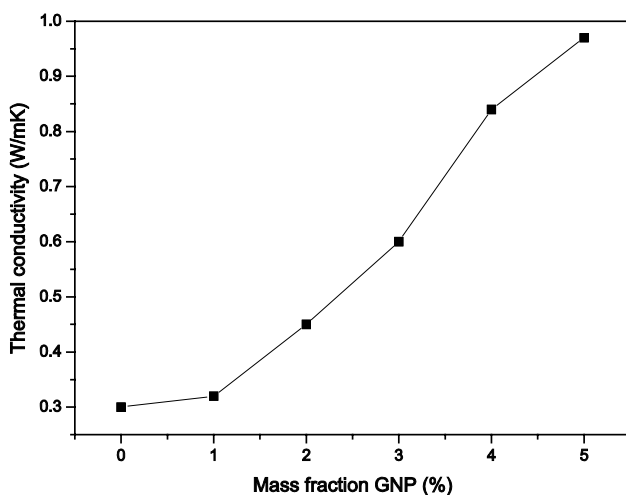


Fig. 7 Thermal conductivity of neat PVDF and PVDF/PMMA/GNP composites with various GNP loadings

found that the thermal conductivity of the composites is enhanced by increasing GNPs content. This indicates a new way to obtain dielectric materials with high thermal conductivity and dielectric constant.

Acknowledgements The work was supported by National Natural Science Foundation of China (Nos. 51607109, 51476094, 51590901), the Natural Science Foundation of Shanghai (Nos. 15ZR1417100, 16ZR1412400), the Popular Science Propaganda on Innovation and entrepreneurship for college students—new energy and new materials (No. 16DZZ348700).

References

1. M.K. Mohanapriya, K. Deshmukh, K. Chidambaram, M.B. Ahamed, K.K. Sadasivuni, D. Ponnamma, M.A. AlMaadeed, R.R. Deshmukh, S.K.K. Pasha, *J. Mater. Sci.* **28**, 6099 (2017)
2. F. Xia, Z.Y. Cheng, H.S. Hu, H.S. Li, Q.M. Zhang, *Adv. Mater.* **14**, 1600 (2002)
3. Z.M. Dang, L.Z. Fan, Y. Shen, C.W. Nan, *Chem. Phys. Lett.* **369**, 95 (2003)
4. K. Deshmukh, M.B. Ahamed, R.R. Deshmukh, S.K.K. Pasha, K.K. Sadasivuni, A.R. Polu, D. Ponnamma, M.A. AlMaadeed, K. Chidambaram, *J. Mater. Sci.* **28**, 973 (2017)
5. K. Deshmukh, M.B. Ahamed, A.R. Polu, K.K. Sadasivuni, S.K.K. Pasha, D. Ponnamma, M.A. AlMaadeed, R.R. Deshmukh, K. Chidambaram, *J. Mater. Sci.* **27**, 11410 (2016)
6. W.Y. Zhou, Y. Gong, L.T. Tu, L. Xu, W. Zhao, J.T. Cai, Y.T. Zhang, A.N. Zhou, *J. Alloy. Compd.* **693**, 1 (2017)
7. K. Deshmukh, M.B. Ahamed, K.K. Sadasivuni, D. Ponnamma, R.R. Deshmukh, A.M. Trimukhe, S.K.K. Pasha, A.R. Polu, M.A. AlMaadeed, K. Chidambaram, *J. Polym. Res.* **24**, 27 (2017)
8. J. Su, J. Zhang, *J. Mater. Sci.* **28**, 5250 (2017)
9. K. Deshmukh, M.B. Ahamed, R.R. Deshmukh, S.K.K. Pasha, K.K. Sadasivuni, D. Ponnamma, K. Chidambaram, *Eur. Polym. J.* **76**, 14 (2016)
10. K. Deshmukh, M.B. Ahamed, S.K.K. Pasha, R.R. Deshmukh, P.R. Bhagat, *RSC Adv.* **76**, 61933 (2015)
11. K. Deshmukh, M.B. Ahamed, K.K. Sadasivuni, D. Ponnamma, M.A. AlMaadeed, S.K.K. Pasha, R.R. Deshmukh, K. Chidambaram, *Mater. Chem. Phys.* **186**, 188 (2017)
12. L.L. Zhang, R. Zhou, X.S. Zhao, *J. Mater. Chem.* **20**, 5983 (2010)
13. H. Xu, J. Liu, Y. Chen, C.L. Li, J. Tang, Q. Li, *J. Mater. Sci.* doi:10.1007/s10854-017-6842-5
14. J.W. Gu, X.T. Yang, Z.Y. Lv, N. Li, C.B. Liang, Q.Y. Zhang, *Int. J. Heat. Mass. Transf.* **92**, 15 (2016)
15. C. Liu, Z. Yu, D. Neff, A. Zhamu, B.Z. Jang, *Nano Lett.* **10**, 4863 (2010)
16. M.H. Al-Saleh, S.A. Jawad, *J. Electron. Mater.* **45**, 7 (2016)
17. E.V. Kuvardina, L.A. Novokshonova, S.M. Lomakin, S.A. Timan, I.A. Tchmutin, *J. Appl. Polym. Sci.* **128**, 1417 (2013)
18. K. Jurczuk, A. Galeski, M. Mackey, A. Hiltner, E. Baer, *Colloid. Polym. Sci.* **293**, 1289 (2015)
19. V. Panwar, K. Cha, J. Park, S. Park, *Sensor. Actuat. B* **161**, 460 (2012)
20. R. Baskaran, S. Selvasekarapandian, N. Kuwata, J. Kawamura, T. Hattori, *Mater. Chem. Phys.* **98**, 55 (2006)
21. A.A. Yousefi, *Iran. Polym. J.* **20**, 109 (2011)
22. M. Abdelaziz, *J. Mater. Sci.* **24**, 2727 (2013)
23. W. Ma, J. Zhang, X. Wang, S. Wang, *Appl. Surf. Sci.* **253**, 8377 (2007)

24. D.D. Yang, H.P. Xu, Y.H. Wu, J.R. Wang, Z.P. Xu, W. Shi, J. Polym. Res. **20**, 236 (2013)
25. K. Deshmukh, M.B. Ahamed, K.K. Sadasivuni, D. Ponnamma, R.R. Deshmukh, S.K.K. Pasha, M.A. AlMaadeed, K. Chidambaram, J. Polym. Res. **23**, 159 (2016)
26. K. Deshmukh, M.B. Ahamed, R.R. Deshmukh, S.K.K. Pasha, K. Chidambaram, K.K. Sadasivuni, D. Ponnamma, M.A. AlMaadeed, Polym. Plast. Tech. Eng. **55**, 1240 (2016)
27. J. Kressler, R. Schafer, R. Thomann, Appl. Spectrosc. **52**, 1269 (1998)
28. M.G. Bachmann, J.L. Koenig, J.B. Lando, J. Appl. Phys. **50**, 6106 (1979)
29. K. Deshmukh, M.B. Ahamed, R.R. Deshmukh, S.K.K. Pasha, K.K. Sadasivuni, D. Ponnamma, M.A. AlMaadeed, J. Mater. Sci. **28**, 559 (2017)
30. B.Y. Newman, K.D. Pae, J.I. Scheinbeim, J. Appl. Phys. **50**, 6095 (1979)
31. A.J. Lovinger, Macromolecules **15**, 40 (1982)
32. C. Wu, X.Y. Huang, L. Xie, X. Wu, J. Yu, P.K. Jiang, J. Mater. Chem. **21**, 17729 (2011)